Infection, Genetics and Evolution 74 (2019) 103922

Contents lists available at ScienceDirect

Infection, Genetics and Evolution

journal homepage: www.elsevier.com/locate/meegid

Research paper

Integration analysis of a miRNA-mRNA expression in A549 cells infected with a novel H3N2 swine influenza virus and the 2009 H1N1 pandemic influenza virus

Lingxi Gao[1], Jie Gao[1], Ying Liang[1], Rui Li, Qing Xiao, Zengfeng Zhang, Xiaohui Fan*

Department of Microbiology, Guangxi Medical University, 22 Shuangyong Road, Nanning 530021, Guangxi, China

ARTICLE INFO

Keywords:
Novel reassortment swine influenza virus
2009 H1N1 pandemic influenza virus
miRNA-mRNA integrated analysis
Microarray
High throughput sequencing

ABSTRACT

Swine are reservoirs for anthropogenic/zoonotic influenza viruses, and the prevalence and repeated introduction of the 2009 H1N1 pandemic influenza virus (pdm/09) into pigs raises the possibility of generating novel swine influenza viruses with the potential to infect humans. However, studies aiming to identify miRNAs involved in the transfer of novel swine influenza virus infection to human cells are rare. In this investigation, from the view of small RNA, microarrays and high-throughput sequencing were used to detect differentially expressed miRNAs and mRNAs after human lung epithelial cells were infected with the following three stains of influenza viruses: a novel H3N2 swine influenza virus reassorted with pdm/09 fragments, pdm/09 and classical swine influenza virus. A miRNA-mRNA interaction map was generated to show the correlation between miRNAs related to infection by the viruses with human infective potential/capability. The expression of 4 miRNAs (hsa-miR-96-5p, hsa-miR-140-5p, hsa-miR-30a-3p and hsa-miR-582-5p) and 5 relevant mRNAs (RCC1, ERVFRD-1, RANBP1, SCARB2 and RPS29) was determined. The integration analysis indicated that these candidates have rarely been reported to be associated with influenza virus. Focusing on miRNA expression changes could reveal novel reassortant viruses with human infective potential that may provide insight into future pandemics.

1. Introduction

The 2009 H1N1 pandemic influenza virus (pdm/09) caused the 2009 pandemic, which was the first influenza pandemic of the 21st century. This swine-origin virus was generated via multiple reassortments of swine, human and avian influenza viruses (Garten et al., 2009; Smith et al., 2009). Pdm/09 not only infects humans but also infects swine and further reassorts with the enzootic swine influenza virus (SIV) (Pereda et al., 2010; Weingartl et al., 2010). New gene reassortant viruses with gene segments of pdm/09 and other SIVs have repeatedly occurred in Eurasia, North America and Southern China, indicating that swine-origin pdm/09 can be passed back to swine after human epidemics and become a component of the SIV gene pool (Ducatez et al., 2011; Howard et al., 2011; Kitikoon et al., 2011; Starick et al., 2011). Pigs are considered intermediate hosts and "mixing vessels," facilitating the genesis of pandemic influenza viruses, as demonstrated by the emergence of pdm/09. If a novel virus is generated via reassortment between pdm/09 and other influenza A viruses in pigs, other animal species or even humans, such a virus might possess high transmissibility in addition to causing high mortality (Ma et al., 2011). Our previous study found that over 50% of the pigs tested positive for pdm/09-like viruses. More importantly, we isolated and identified several strains that were reassorted with H3N2 SIVs and pdm/09 in Guangxi Province, China between 2010 and 2014 (Fan et al., 2012; Liang et al., 2014). One swine virus, i.e., A/Swine/Guangxi/NS2783/2010(H3N2) (SW2783), infected humans potentially because the genetic analysis of SW2783 hemagglutinin (HA) and neuraminidase (NA) genes showed that these genes clustered together and were closely related to an H3N2 swine virus as represented by Swine/Binh Duong/03_06/2010. This virus had seasonal human virus-like surface genes and TR-like internal genes and was isolated from a two-year-old girl in Vietnam in February 2010 (Ngo et al., 2012). In addition, the six internal genes of SW2783 originate from pdm/09. Animal experiments have shown that this virus is effectively transmitted from pig to ferret and can replicate in ex vivo human lung tissue. The continuing prevalence of the pdm/09 virus in pigs could lead to the genesis of novel swine reassortment viruses with the potential to infect humans.

Therefore, research should focus on infection by new reassortant

* Corresponding author.
E-mail address: fanxiaohui63@163.com (X. Fan).
[1] The first three authors contributed equally to this paper.

https://doi.org/10.1016/j.meegid.2019.103922
Received 9 April 2019; Received in revised form 29 May 2019
Available online 14 June 2019

viruses in terms of both the evolution of viruses and the development of infection. MicroRNAs (miRNAs) are small endogenous (21–23 nucleotides), noncoding RNAs that are highly conserved and control the translation and transcription of their target genes through the RNA interference pathway. These molecules play important roles in the regulation of various biological processes and viral infection. Several previous studies have reported an interactional correlation between miRNA profile alterations and influenza virus infections with various models, such as different types of cells, patient serum samples or throat swabs, and multiple kinds of mammals (Loveday et al., 2012; Lam et al., 2013; Wu et al., 2013). However, due to the diversity in the study methods or models, the results lack a uniform trend, and because of a wide range of miRNAs, more evidence is needed , thus, the miRNAs associated with the infection of the emergent H3N2 SIV as a virus with human infective potential/capability are unclear. Therefore, in this study, we used reassorted H3N2 SIV (A/Swine/Guangxi/NS2783/2010(H3N2), SW2783), the 2009 H1N1 pandemic influenza virus (A/California/07/09(H1N1), CA09) and a classical H1N1 SIV (A/Swine/Guangxi/3861/2011(H1N1), SW3861) to infect human lung epithelial cells (A549). SW2783 is a virus with human infective potential, and its gene reassorted the H3N2 SIV surface gene and pdm/09 internal genes. CA09 is the vaccine strains of pdm/09 recommended by the WHO. SW3861 is a classical swine H1N1 influenza virus that never recombined with any extraneous lineages since infecting pigs in 1978. SW3861 is less likely to accomplish cross-species infection in humans (Liang et al., 2014). The miRNAs and mRNAs were extracted and then used in miRNA microarrays and transcriptome sequencing during the acute stage of infection after 24 h. We identified several aberrantly expressed miRNAs in the SW2783 and CA09 infection groups. By performing an interaction analysis of the miRNA-mRNA network and a Gene Ontology (GO)/Kyoto Encyclopedia of Genes and Genomes (KEGG) enrichment function analysis, these candidate miRNAs and relevant mRNAs were presumed to play certain roles in influenza virus infection. This finding demonstrates that global miRNA and related transcription profiling is an innovative strategy for uncovering new sensitive measures of response to novel reassortant SIV infection in humans. The differential response signatures obtained in our data are indicative of certain miRNAs that may play an important role in regulating influenza virus with human infective potential/capability.

2. Results

2.1. Analysis of common miRNA and mRNA profiles in response to influenza virus infection

To investigate the changes in the host gene expression profile occurring during influenza virus infection in humans, the global cellular miRNA expression patterns in A549 cells infected with the influenza virus strains SW2783, SW3861 and CA09 were compared with those in uninfected cells (negative control, NC). We defined the differential expression of miRNAs based on normalized reads according to the criteria of a fold change > 2.0 and a P-value < .05.

The miRNAs were identified and classified as upregulated and downregulated in comparison to the miRNA levels in the uninfected cells. Compared with the NC, 53 miRNAs were differentially expressed in A549 cells infected with SW2783, including 17 upregulated and 36 downregulated miRNAs. 63 miRNAs were differentially expressed in the sample infected with CA09, including 26 upregulated and 37 downregulated miRNAs. 35 miRNAs were differentially expressed in the sample infected with SW3861, including 11 upregulated, and 24 downregulated miRNAs. The variation in the miRNA expression levels is demonstrated by volcano plots (Supplementary Fig. S1a). Hierarchical clustering was conducted to cluster the differentially expressed miRNAs (DEMs), each sample was subjected to triplicate analyses, and the results are shown by heat maps (Supplementary Fig. S1b). As shown in the volcano plots and heat maps, comparing with the NC, most miRNAs were downregulated, especially groups infected with SW2783 and CA09, and the number of downregulated miRNAs were comparable (Supplementary Fig. S3a).

Table 1
The numbers of differentially expressed miRNAs and mRNAs in different infected groups compared with the uninfected group.

Different infected groups	Up-regulated		Down-regulated	
	miRNA	mRNA	miRNA	mRNA
SW2783 vs NC	17	1491	36	643
SW3861 vs NC	11	1326	24	548
CA09 vs NC	26	2197	37	1365

The identification of differentially expressed genes (DEGs) between the infected and uninfected groups was performed on the basis of a fold change > 2.0 and a P-value < .05. The volcano plot and heat map based on gene expression (Supplementary Fig. S2) indicate the SW2783 infection increased the expression of 1491 DEGs and decreased the expression of 643 DEGs, while the CA09 infection upregulated 2197 and downregulated 1365 DEGs. Additionally, 1874 DEGs were differentially regulated by SW3861, including 1326 up- and 548 downregulated DEGs. This finding suggests that different gene regulation characteristics exist among influenza virus strains with different virulence and species (Supplementary Fig. S3b). The numbers of DEMs and DEGs are displayed in Table 1.

2.2. Cellular miRNAs and transcriptome signatures in response to the pandemic 2009 H1N1 (CA09) and the novel reassortant virus (SW2783) infection in A549 cells

As a novel reassortant swine virus with segments of pandemic 2009 H1N1, SW2783 has the ability of trans-species infection of humans; however, as a classic swine virus with a conserved gene, SW3861 can hardly establish effective infection and transmission to humans. Therefore, it is assumed that certain small RNAs produced by host cells participate in the viral infection with human infective potential/capability. To identify these small RNAs, a Venn diagram was generated to display the DEMs and DEGs among the SW2783, CA09 and SW3861 infection groups compared to the NC. The DEMs that were present in SW2783 and CA09 groups but absent in SW3861 group were identified as the list of interest. As shown in the Venn diagram (Fig. 1a, red circle), 19 downregulated and 9 upregulated miRNAs were identified in SW2783 infection group. However, these miRNAs were differentially regulated by the three strains of viruses with various genetic reassortment and infective affinity levels (Fig. 1b). All selected DEMs (uniquely present in SW2783, uniquely present in CA09, and present in both SW2783 and CA09) are shown in Fig. 2a, and the pattern of the DEMs was similar between SW2783 and CA09 (Fig. 2b). While focusing on the DEGs during infection, following the same selection criteria, 514 up- and 253 downregulated DEGs were present in SW2783 group. Accordingly, the expression of 344 DEGs was significantly altered in SW2783 and CA09 groups (Fig. 1a). The DEMs and DEGs profiles in the infections are shown (Fig. 1b). In total, 52 DEMs and 2543 DEGs were present in SW2783 and CA09 groups, which have the ability or potential of human infection, but absent in SW3861 group, which is not capable of human infection (Fig. 1a).

2.3. Functional annotation and pathway enrichment analysis of DEGs during infection

Three databases (TargetScan, microRNAorg, and PITA) were used to predict the target genes of 52 candidate miRNAs, and the 2543 candidate mRNAs of SW2783 and CA09 infection were in the predicted set of target genes. Subsequently, to clarify the regulatory pathways and functions of the miRNAs in humans in response to influenza virus

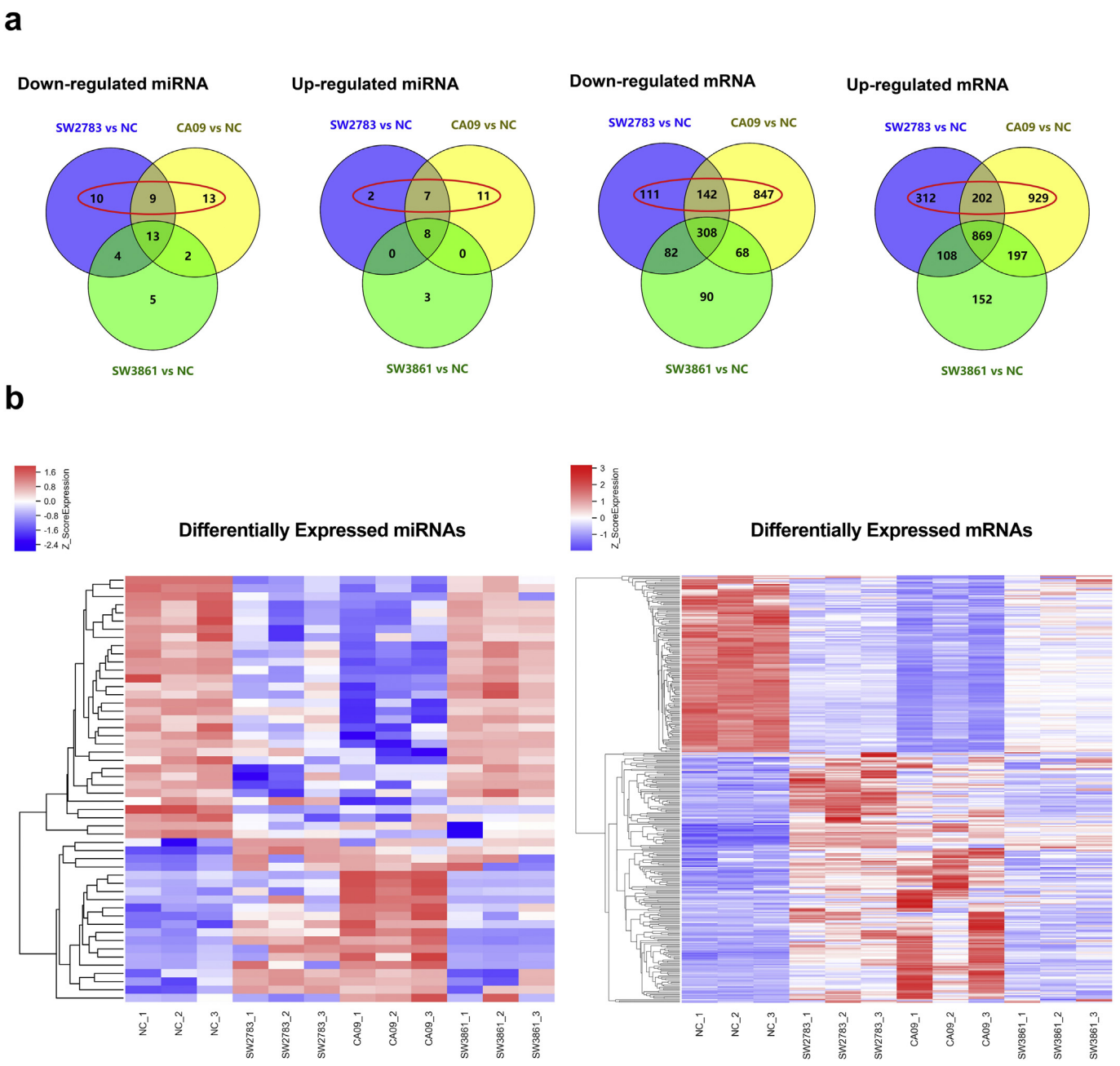

Fig. 1. Specific differentially expressed miRNAs and mRNAs during infection. a. A Veen diagram was generated to display the differentially expressed miRNAs and mRNAs uniquely present in SW2783, uniquely present in CA09, and present in both SW2783 and CA09 compared to the NC in lists of interest for infection. (red circle). b. Heap map of all differentially expressed miRNAs and mRNAs regulated by three strains of viruses. All experiments (n = 3) were performed in triplicate. (For interpretation of the references to colour in this figure legend, the reader is referred to the web version of this article.)

infection, the intersectional DEGs in infection were subjected to a gene functional analysis. To further characterize the roles of the mRNAs differentially expressed during SW2783 and CA09 infection, GO (http://www.geneontology.org/) and KEGG (https://www.kegg.jp/) pathway annotations were performed using R language to explore the distribution and potential biological functions of these candidate target genes. The GO method divides all genes into the following three classifications: biological process (BP), cellular component (CC) and molecular function (MF). According to the GO terms assigned to the target mRNAs identified in this study, we analyzed the top 10 significantly enriched GO terms among the three classifications (Fig. 3a), and these target mRNAs were involved in all three categories ($P < 0.05$). Among these processes, in the BP classification, the terms related to the target mRNAs during virus infection included viral transcription, which showed a very high enrichment (top 2, $P < 0.05$), and the candidates included RPS10, RPS12, RPS29, RPLP1, RPS17, RPS28 and RPS21, all of which are components or functional genes of the ribosome (Kenmochi et al., 1998; Mirabello et al., 2014). This interesting finding indicates that the ribosome might play a significant role during viral transcription in infection induced by the influenza viruses, which have the ability to infect human cells. The CC GO terms further support our results as small ribosomal subunit ($P < 0.01$) and cytosolic small ribosomal subunit ($P < 0.01$) were significantly enriched and involved in the DEGs RPS10, RPS12, RPS29, RPS17, RPS28, RPS21, RPS29, RPS28 and RPS21. Additionally, the viral envelope ($P < 0.01$) was distinctly enriched, and ERVFRD-1 (Morozov et al., 2013) was involved (not shown in the top 10 GO terms). In summary, the DEGs related to viral transcription and the viral envelope have high specificities and

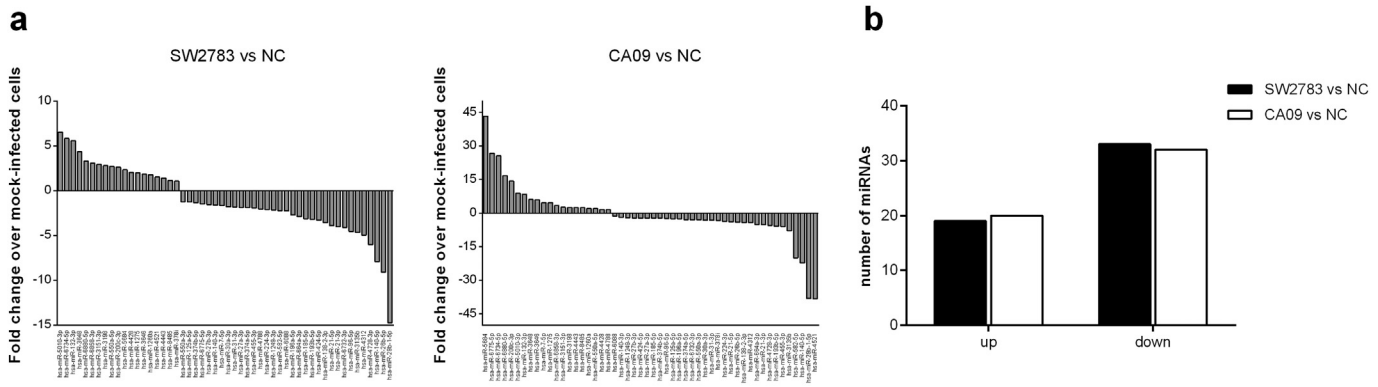

Fig. 2. Strain-specific differentially expressed miRNAs induced by SW2783 and CA09. a. Strain-specific differentially expressed miRNAs regulated by SW2783 and CA09 during the acute infection (24 h). b. Numbers of abnormally expressed miRNAs in SW2783 and CA09 compare with the NC. Variation tendency of specific DEMs was similar in both SW2783 and CA09 infection.

were correlated with A549 cell infection by SW2783 and CA09. The candidate targets involved in the most important genetic information processing, environmental information processing and cellular processes were identified using KEGG pathway mapping. The selected DEGs were imported into KEGG databases, and 271 pathway terms were produced. The 20 most prominent KEGG pathways ($P < 0.05$) were identified (Fig. 3b). The immune-related pathway, metabolism and ribosome were the most represented subunits among these groups. Complement and coagulation cascades, the ribosome, and the metabolism of certain amino acids were implicated. The significant enrichment of the ribosome in the KEGG pathways analysis shows the same results as the GO terms analysis, which suggests that during viral transcription, some genes in the ribosome pathway may play an important role in response to the invasion of influenza viruses with human infective potential/capability.

2.4. Integrated network of the host cell miRNA-mRNA interactome

An interaction network analysis of miRNAs and mRNAs was performed as follows: we focused on strain-specific differentially expressed small RNAs induced by SW2783 and CA09 (viruses with human infective potential/capability). In total, 10 DEGs were associated with viral infection or host antiviral responses in the analysis of the GO function annotations and KEGG pathway enrichment. These DEGs, namely, ANPEP, ERVFRD-1, ANBP1, RCC1, RPLP1, RPS21, RPS28, RPS29, SCARB2 and TRIM27, were identified on the basis of Venn diagram selection (Fig. 1a). These selected DEGs mainly participate in biological processes, including the GO terms viral transcription, negative regulation of the adaptive immune response, signal transduction, and viral envelope; CC, including the GO term small ribosomal subunit; and the KEGG pathways ribosome, host defense inflammatory immune response, metabolism, and transcription. A PPI map was constructed to perform a conjoint analysis of the 10 DEGs and their relevant miRNAs, and these miRNAs were examined as candidates in a Venn diagram selection of differentially expressed miRNAs (Fig. 1a). As shown in the PPI map (Fig. 4), 34 of 52 miRNAs targeting 10 mRNA pairs were identified. Some miRNAs targeted more than one mRNA, such as hsa-miR-582-5p, which targets RCC1, TRIM27, RPS29 and SCARB2, and hsa-miR-140-5p, which targets ERVFRD-1 and SCARB2. Accordingly, several miRNAs played roles in multiple pathways. For example, hsa-miR-582-5p and hsa-miR-96-5p were involved in the negative regulation of the adaptive immune response and interferon-gamma secretion in the BP, and these molecules also belong to the ribosome pathway. Additionally, we analyzed the expression level of these relevant miRNAs based on a miRNA microarray of all three virus infections and examined whether these 34 miRNAs meet the screening requirements of DEMs in the microarray. Eight miRNAs targeting 10 mRNA pairs were chosen for further validation.

2.5. Validation of miRNA and mRNA expressions by quantitative RT-PCR and selection analyses

In total, we selected 8 miRNAs, namely, hsa-miR-96-5p, hsa-miR-140-5p, hsa-miR-196a-5p, hsa-miR-224-3p, hsa-miR-30a-3p, hsa-miR-664a-3p, hsa-miR-582-5p and hsa-miR-200c-3p, for the validation. After quantitative RT-PCR, we constructed a histogram of the relative expression ratio of 8 miRNAs between SW2783, CA09 and SW3861 (SW2783/SW3861, CA09/SW3861) as shown in Fig. 5a. A relative expression ratio change ≤ 0.67 or ≥ 1.5 was considered to have a high confidence level. Four miRNAs (hsa-miR-96-5p, hsa-miR-140-5p, hsa-miR-30a-3p and hsa-miR-582-5p) met this requirement in both SW2783 and CA09 infection, indicating that 4 miRNAs were significantly expressed in the SW2783 and CA09 infections than SW3861 infection. A quantitative expression analysis of these 4 miRNAs was performed (Fig. 5b), and the statistical analysis (paired *t*-test) showed that all four miRNAs were significant in the influenza virus infection groups compared with the NC ($P \leq 0.05$). The validation by quantitative RT-PCR was consistent with the microarray results. Moreover, by performing the integrated analysis of the miRNA-mRNA interaction network, 5 mRNAs were identified as the target genes of the expression of the 4 miRNAs (Table 2). A quantitative RT-PCR analysis was also performed to validate the 5 selected mRNAs (RCC1, ERVFRD-1, RANBP1, SCARB2 and RPS29), and the relative expression is shown in Fig. 5c. The validation of these DEGs was consistent with the sequencing results.

3. Discussion

Our previous research revealed the isolation and genetic characterization of over 10 strains of the novel reassortment of H3N2 swine virus from 2010 to 2014 in Guangxi, China, and these strains have surface genes derived from a seasonal H3N2/triple reassortant (TR) swine virus and internal genes from pdm/09-like viruses. SW2783 has been considered a strain of virus with human infective potential/capability, indicating that SW2783 has the ability to establish the cross-species infection in humans (Fan et al., 2012). This is considered a special process of infection induced by viruses with human infective potential/capability, where miRNAs may play important roles. Therefore, this research focuses on the global host response to infection caused by novel reassortant SIVs and a pandemic strain, with the emphases on the correlation between influenza virus infection and miRNA expression changes in host cells.

To answer this question, we performed an integration analysis of differentially expressed miRNAs and mRNAs involved in the following three strains of influenza virus infected in the A549 cells at an acute

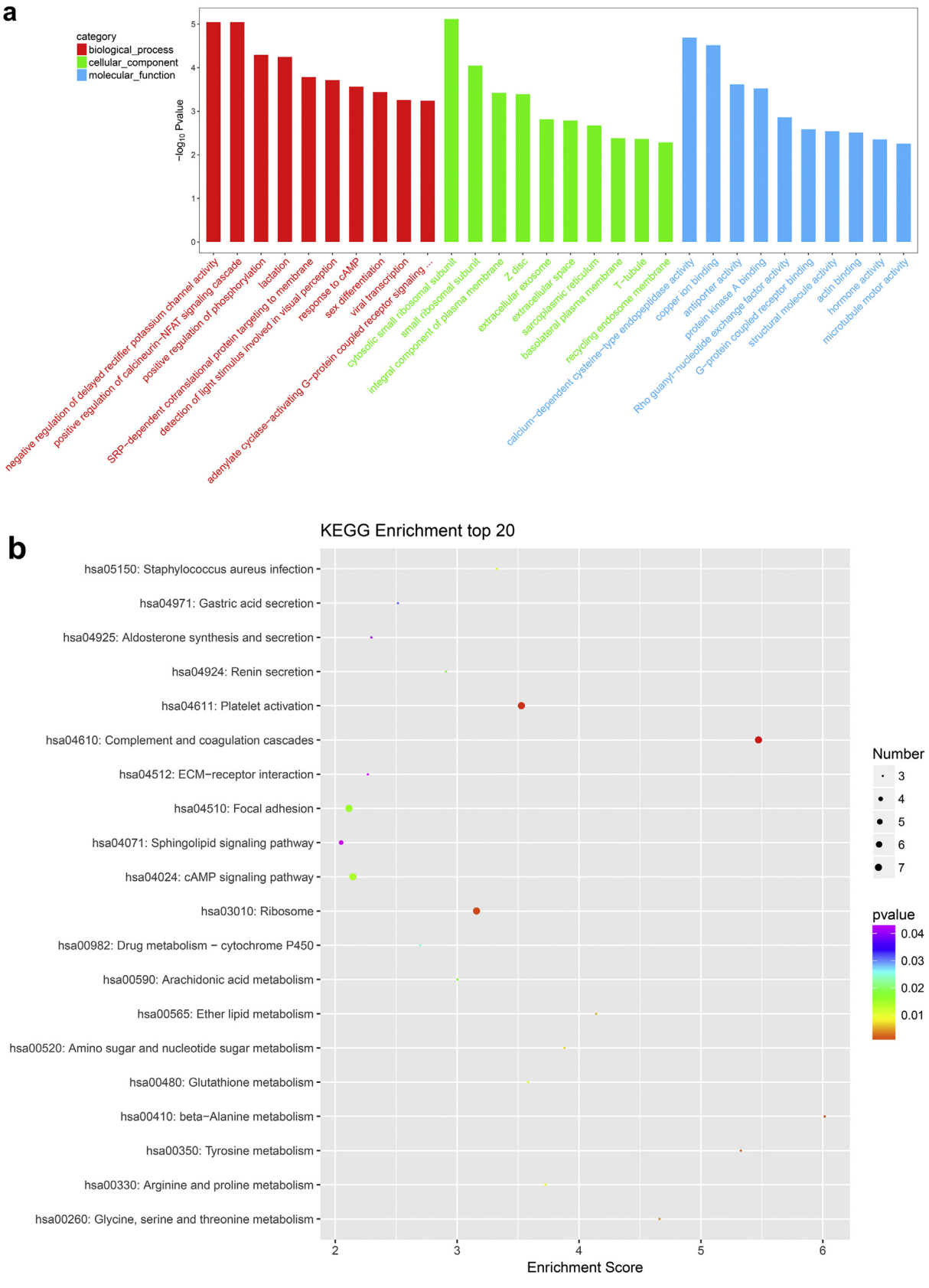

Fig. 3. GO and KEGG analyses of differentially expressed mRNAs in infection with viruses with human infective potential/capability. a Bar diagram displaying the top 10 GO terms in each category (ListHits > 2 and sort by -log10P-value from high to low, $P < 0.05$) and significant differences in the differentially expressed mRNAs. b KEGG enrichment analysis of each of the top 20 significantly different differentially expressed mRNAs. The bubble diagram displays the top 20 items (ListHits > 2 and sort by -log10P-value from high to low, $P < 0.05$).

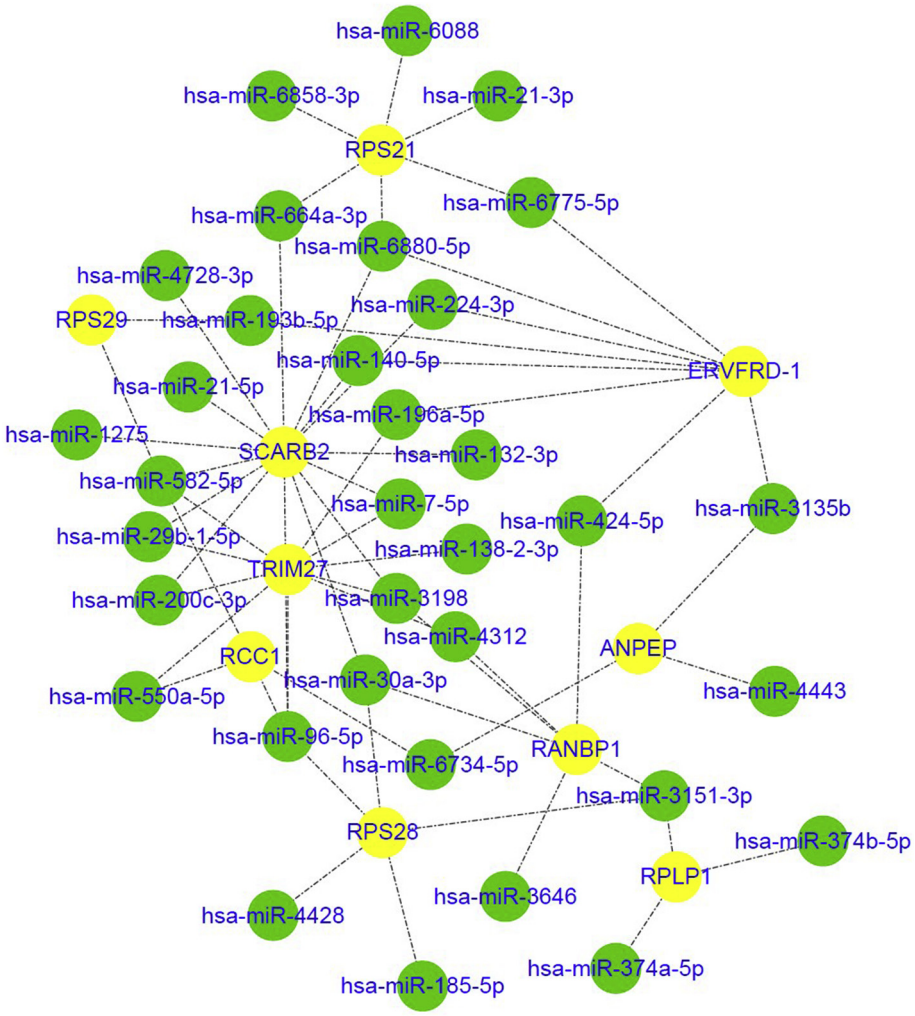

Fig. 4. Conjoint analysis of a DEMs and DEGs integrated network in the infection. Yellow circles represent the abnormal changed DEGs, and green circles represent the miRNAs that target those genes. (For interpretation of the references to colour in this figure legend, the reader is referred to the web version of this article.)

infection time point (24 h): SW2783, a novel reassortant H3N2 swine virus with internal genes from pdm/09-like virus; CA09, a vaccine strain of the pandemic 2009 H1N1 influenza virus; SW3861, a classical H1N1 swine virus with a low potential of human infection. In total, 52 miRNAs and 2543 related mRNAs were significantly differentially expressed in human lung epithelial cells infected by SW2783 and CA09 compared to those infected by SW3861. The expression of 4 miRNAs and 5 relevant mRNAs were verified and they are consistent with microarray and high-throughput sequencing. In addition, an interaction analysis was performed to describe their relationship and potential functions by GO term and KEGG pathway analyses, and the results indicated that these miRNAs are stimulated by 'human-infecting' viruses

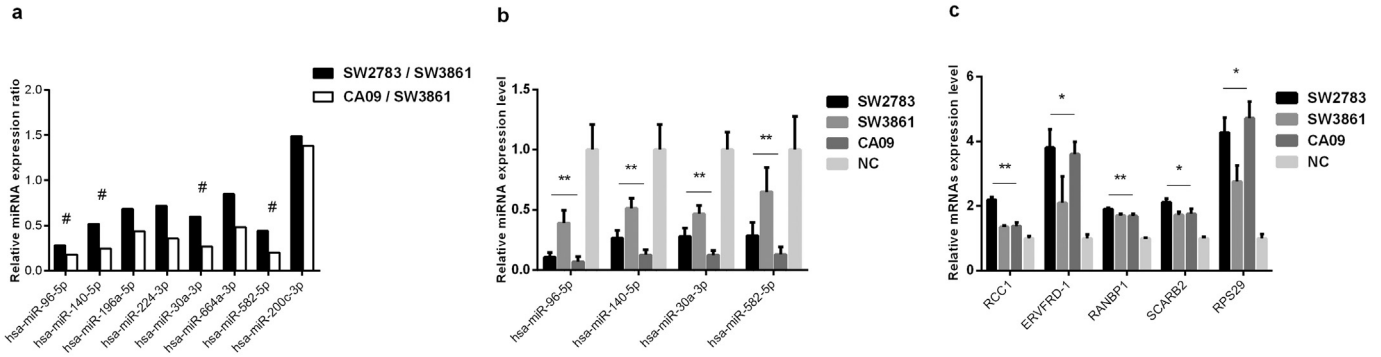

Fig. 5. Validation by RT-qPCR of the differentially expressed miRNAs and mRNAs in infection. a. Histogram of the relative expression ratio of 8 miRNAs among SW2783, CA09 and SW3861 (SW2783/SW3861, CA09/SW3861); a relative expression ratio change ≤0.67 or ≥1.5 is considered as the high confidence. # Ratio ≤ 0.67. b and c. Quantitative expression analysis of 4 miRNAs and 5 relative mRNAs. The level of expression in the uninfected samples is set to one, and the relative expression values were normalized to internal standards. The data are expressed as the means ± SD. All experiments (n = 3) were performed in triplicate. * $P \leq 0.05$, ** $P \leq 0.01$, statistical analysis was performed using one-way ANOVA.

Table 2
Relationships between 4 miRNAs and 5 inversely correlated target genes selected in qRT-PCR.

miR_name	Regulation	Target gene
hsa-miR-96-5p	Down	RCC1, SCARB2
hsa-miR-140-5p	Down	ERVFRD-1, SCARB2
hsa-miR-30a-3p	Down	RANBP1, SCARB2
hsa-miR-582-5p	Down	RCC1, RPS29, SCARB2

that have rarely been reported to be affiliated with influenza virus. This finding may indicate that some miRNAs could be sensitive measures of the host response to acute infection by viruses with human infective potential/capability.

Previous studies investigating the same abnormally expressed miRNAs found in our study were summarized and reviewed. The expression of miR-140-5p decreases during the infection with EV71(human enterovirus 71) and RSV (respiratory syncytial virus pneumonia) and, can affect the inflammatory response and immunoreaction (Cui et al., 2011; Zhang and Shao, 2018). Several studies found that the decreased expression of miR-30a-5p could benefit the viral replication in EV71 and HCV (hepatitis C virus) infection (Fu et al., 2015; El-Ekiaby et al., 2017). Our results showed similar trends in performance changes as follows: the expression of miR-140-5p and miR-30a-5p decreased significantly in the SW2783 and CA09 infection groups compared with that in the SW3861 or NC, suggesting that expression of these two miRNAs were more highly suppressed in human cells after infection of viruses with human infective potential/capability. The overexpression changes of miR-96 in HBV (hepatitis B virus), HSV (herpes simplex virus) and HCMV (human cytomegalovirus) have been identified (Stark et al., 2012; Majer et al., 2017; Singh et al., 2018). Intriguingly, the expression of miR-96 was upregulated in most previous studies. In contrast, miR-96-5p was downregulated in the influenza virus infection in the current research, indicating that the regulation of miR-96-5p expression in infection with influenza viruses with human infective potential/capability differs from that infection with other viruses. The transfection of miR-582 enhanced staurosporine and TNF-α-induced apoptosis and affected genes related to apoptotic pathways (Shen et al., 2018). Nevertheless, studies investigating the involvement of miR-582 in viral infection are rare; Tuddenham reported that human herpesvirus 6 may encode viral miRNAs and one of them is a seed ortholog of the human miRNA miR-582-5p (Tuddenham et al., 2012). Our results show that the downregulation of miR-582-5p during influenza virus infection was a remarkable change specifically induced by influenza viruses with human infective potential/capability. This study was the first to reveal that miR-582-5p is involved in the interaction between viral invasion and human cells. However, whether the decreased expression of such miRNAs will could benefit viral infection or enhance host antiviral responses in influenza virus infection are is still worthy of further investigation is needed.

The functional analysis of the related DEGs was performed according to the statistical computing of GO terms and KEGG pathways after obtaining the miRNAs and mRNAs from the three influenza virus infection groups. SCARB2 belong to scavenger receptor class B and has virus receptor activity. SCARB2 has already been confirmed to be a cellular receptor for EV71 and coxsackie viruses A7, A14, and A16 (Yamayoshi et al., 2012). In addition, the overexpression of SCARB2 in cells can significantly enhance EV71 and HCV replication and infectivity (Li et al., 2013) (Grove et al., 2007). SCARB2 has been found to participate in the biological process of 'viral entry into the host cell' in the GO term analysis in our study. Therefore, SCARB2 may regulate the process of influenza virus entry into the host cell in the endosome (Czabotar et al., 2004; Samji, 2009). All 4 DEMs could regulate SCARB2, indicating that this regulation might be involved in complicated interacting networks. In addition to SCARB2, the ERVFRD-1(Endogenous retrovirus group FRD envelope protein member 1) gene also mediates viral fusion with host cell membranes and is implicated in the biological process involving the GO term "syncytium formation" based on our results. ERVFRD-1 can induce cell-cell fusion when expressed in cells possessing appropriate receptors (Blaise et al., 2003). Endogenous envelope proteins can make pseudo types with MLV, HIV-1 or SIV-1 virions, confer infectivity, and mediate receptor recognition and membrane fusion during early viral infection (Blaise et al., 2004). In addition, endogenous envelope proteins can suppress T-cell proliferation and LPS-induced TNF-α and IL-12 release (Hummel et al., 2015), which may increase the ability of viral infection. Our results suggest that ERVFRD-1 may facilitate influenza virus invasion into human cells by mediating the fusion of the viral and the cell membrane or, by reducing the host antiviral immune response, yet more evidence is needed to support this hypothesis. The 'human-infecting' viruses may stimulate host cells, resulting in the production of particular miRNAs or infection enhancement by miRNA and mRNA interaction networks. In addition, the proteins encoded by the two membrane fusion function genes (SCARB2 and ERVFRD-1) attracted our attention. The function of the 40S ribosomal protein S29 (RPS29) during influenza virus infection also worth exploration. This gene encodes a protein which is a component of the small 40S ribosomal subunit and is essential for rRNA processing and ribosomal biogenesis (Kenmochi et al., 1998). The expression of RPS29 gene in the SW2783 group was the highest compared with that of the other 4 DEGs. Interestingly, a previous study showed that the content of the S29 protein in the ribosomes of A549 cells was distinctly low (Zhou et al., 2003). As a 40S ribosomal subunit, RPS29 can affect the protein synthesis, such as the synthesis of Polymerase II (Pol II) and some viral proteins(including PB2, PB1, PA and NP protein), which are obligatory for viral transcription (Martinez-Alonso et al., 2016; Bauer et al., 2018; Oymans and Te Velthuis, 2018). RPS29 has been postulated to participate in the gene transcription of influenza viruses, and the BP of RPS29 was enriched in "viral transcription" according to the GO term analysis. According to the target gene prediction results, we focused on the regulatory network and the effects of hsa-miR-582-5p and hsa-miR-140-5p and their target genes. Functional experiments investigating the specific pathways of hsa-miR-582-5p and hsa-miR-140-5p could represent a future research endeavor. It is possible that hsa-miR-582-5p and hsa-miR-140-5p are potential noteworthy biomarkers of infection with influenza viruses with human infective potential/capability.

The other two candidate mRNAs, RCC1 (regulator of chromosome condensation 1) and RANBP1 (Ran-specific binding protein 1), were both regulatory factors of the small GTPase Ran enzyme. However, RCC1 and RANBP1 are believed to have opposite functions in viral replication (Plafker and Macara, 2000). It can be speculated that during other virus infection, RCC1 and RANBP1 are in a dynamic change during vRNPs transport between the nucleus and cytoplasm of the host cell (Chen et al., 2014; Deschamps et al., 2017). Surprisingly, the expression of RCC1 and RANBP1 was upregulated in the SW2783 and CA09 infection, implying the relationship between the expression change and viral infection remains ambiguous.

In summary, multiple miRNAs and mRNAs function in the same biological processes, and in the course of host cell invasion by viruses with human infective potential/capability. The interactions of certain miRNAs and mRNAs drive viral replication and infection. The current study performed an overall analysis of miRNA and relevant mRNA profiles by microarray and high-throughput sequencing in human lung epithelial cells infected with three different strains of influenza virus, including one strain with the ability of human infection as a new reassortant SIV. The current study provides biomarkers candidates for the interference or control the influenza virus outbreaks in the human population.

4. Materials and methods

4.1. Virus isolates and cell lines

The influenza viruses A/Swine/Guangxi/NS2783/2010(H3N2) (SW2783), A/Swine/Guangxi/3861/2011(H1N1) (SW3861) and A/California/07/2009(H1N1) (CA09) were maintained in our laboratory. SW2783 was isolated and identified in Guangxi, China in 2010 (Fan et al., 2012). For comparison, a classical SIV H1N1 strain isolated in 2011, i.e., A/Swine/Guangxi/3861/2011(H1N1) (SW3861), and a vaccine strains recommended by the WHO for the pandemic 2009 H1N1 influenza virus, i.e., A/California/07/2009(H1N1) (CA09), were used in this study. All experiments involving live influenza viruses were performed at Guangxi Medical University under biosafety level 3 conditions. Mandin-Darby canine kidney cells (MDCK, ATCC) were maintained in Eagle's Minimal Essential Media (MEM) supplemented with 10% FBS, 100 U/ml penicillin and 100 μg/ml streptomycin (Gibco, Life Technologies). Human lung epithelial cells (A549, ATCC) were maintained in Ham's F-12 medium (Kaign's modification) supplemented with 10% FBS, 100 U/ml penicillin and 100 μg/ml streptomycin (Gibco, Life Technologies). The cells were cultured at 37 °C in a 5% CO_2 incubator. All viruses were titrated by HA titer on 7-day-old chick embryos and the $TCID_{50}$ were tested on MDCK cells, as previously described (Weingartl et al., 2010).

4.2. Virus infections and RNA isolation

A549 cells are widely applied in studies investigating respiratory effects in vitro (Roggen et al., 2006; Kim et al., 2011). It was also commonly used as an in vitro model to study host cellular small RNA changes in response to diverse viral infections. Briefly, the cells were seeded onto T-75 flasks until reaching 80% to 90% confluency in triplicate for each virus. Prior to the viral infection, the flasks were washed with PBS to remove traces of FBS. Confluent A549 cells were infected with influenza viruses at a MOI of 1 (10^6 PFU/ml of SW2783 and 10^5 PFU/ml of SW3861 and CA09) to infect a monolayer of 10^5 cells. After 1 h of infection, the viruses were removed, the cells were washed 3 times with PBS, 2 ml of fresh Ham's F-12 medium supplemented with 100 U/ml penicillin, 100 μg/ml streptomycin and 1 μg/ml L-1-tosylamido-2-phenylethyl chloromethyl ketone (TPCK)-treated trypsin (all from Gibco, Life Technology), and incubated at 37 °C in a 5% CO_2 incubator for up to 24 h post infection (hpi). Then, the supernatant and cells were collected, treated with lysis/binding buffer (Invitrogen, Thermo Scientific) and immediately frozen in liquid nitrogen for the RNA isolation. As the negative control, A549 cells were mock-infected in parallel and processed in same way. The total RNA was isolated using a miRvana miRNA Isolation Kit (Invitrogen, Thermo Scientific) according to the manufacturer's instructions and quantified by the NanoDrop ND-2000 (Thermo Scientific).

4.3. miRNA microarray construction and expression profiling

The RNA integrity was assessed using an Agilent Bioanalyzer 2100 (Agilent Technologies). For miRNA microarray construction, the Agilent Human miRNA Microarray Release 21.0 (8*60 K, Design ID:070156) was used. The sample labeling, microarray hybridization and washing were performed based on the manufacturer's standard protocols (Oebiotech, Shanghai, China). Next, the arrays were scanned with the Agilent G2505C Scanner (Agilent Technologies). Feature Extraction software (version 10.7.1.1, Agilent Technologies) was used to analyze the array images and obtain the raw data. Then, GeneSpring (version 14.8, Agilent Technologies) was employed to complete the basic analysis with the raw data. First, the raw data were normalized with the quantile algorithm. Later, the differentially expressed miRNAs were identified in the infected cells and normalized to those in the uninfected control cells through fold changes and P-values were calculated by using *t*-tests. The threshold for the up- and downregulated genes was set to a fold change > 2.0 and a P-value < .05.

4.4. mRNA sequencing and expression profiling

Samples with RNA Integrity Numbers (RINs) ≥ 7 were subjected to the subsequent analysis. The libraries were constructed using a TruSeq Stranded mRNA LTSample Prep Kit (Illumina, San Diego, US) according to the manufacturer's instructions (Oebiotech, Shanghai, China). These libraries were sequenced on an Illumina sequencing platform (HiSeq™ 2500 or Illumina HiSeq X Ten). The raw data (raw reads) were processed using the NGS QC Toolkit (Makkoch et al., 2016). Reads containing ploy-N and the low-quality reads were removed to obtain clean reads. Then, the clean reads were mapped to the reference genome using hisat2 (Kim et al., 2015). The FPKM (Trapnell et al., 2010) and read count values of each transcript (protein coding) were calculated using Bowtie2 (Langmead and Salzberg, 2012) and eXpress (Roberts and Pachter, 2013). The DEGs were identified using the DESeq R package functions estimateSizeFactors and nbinomTest. A P-value < .05 and a fold change > 2 or < 0.5 were set as the thresholds for significantly differential expression.

4.5. Biological function analysis

For the miRNAs, the target genes of the DEMs were the intersections predicted with databases (TargetScan: http://www.targetscan.org/vert_72/, microRNAorg: http://www.microrna.org/, and PITA: https://genie.weizmann.ac.il/pubs/mir07/mir07_data.html). GO enrichment and KEGG pathway analyses were applied to determine the roles of these target genes. Hierarchical clustering was performed to show the distinguishable miRNA expression patterns among the samples. For the mRNAs, a hierarchical cluster analysis of the DEGs was performed to explore the transcript expression patterns. The GO enrichment and KEGG pathway enrichment analyses of the DEGs were performed using R based on the hypergeometric distribution.

4.6. Correlation analysis of miRNAs and mRNAs

To build a comprehensive miRNA-mRNA network with positive and negative correlations, we constructed a miRNA-mRNA regulatory network. The DEMs and DEGs were collected from the miRNA and mRNA list. Then, we used miRanda (http://www.microrna.org/microrna/home.do), TargetScan and DAVID (https://david.ncifcrf.gov/) to confirm the correlations between the miRNAs and mRNAs. All potential mRNA targets among the assayed protein-coding genes were identified to be associated with miRNAs differentially expressed after virus infection, and we focused on those exclusively expressed in the viruses with human infective potential/capability. Finally, the infecting-human-specific DEMs and related DEGs were verified.

4.7. Quantitative RT-PCR analysis of DEMs and relevant DEGs

To validate the microarray and sequencing data of our candidate miRNAs and mRNAs, quantitative RT-PCR was performed. The total RNA was isolated at 24 hpi after virus infection using the miRvana miRNA Isolation Kit (Invitrogen, Thermo Scientific) according to the instructions and quantified by a NanoDrop ND-2000 (Thermo Scientific). The integrity was evaluated using agarose gel electrophoresis and ethidium bromide staining. RT reactions were performed on a GeneAmp® PCR System 9700 (Applied Biosystems, USA). The real-time PCR analysis was performed using QuantiFast® SYBR® Green PCR Master Mix (Qiagen , Germany) on a LightCycler® 480IIReal-time PCR Instrument (Roche, Swiss). Each sample was run in triplicate for analysis. At the end of the PCR cycles, a melting curve analysis was performed to validate the specific generation of the expected PCR products. The miRNA/mRNA-specific primer were designed based on the

miRNA sequences obtained from the miRBase database (Release 20.0) and the mRNA sequences obtained from the NCBI database (the primers are listed in Supplementary Tables 1 and 2). Primers were synthesized by Generay Biotech (Generay, China). The miRNA expression levels were normalized to U6, and the mRNA expression levels were normalized to ACTB. The expression levels were calculated using the $2^{-\Delta\Delta Ct}$ method.

Supplementary data to this article can be found online at https://doi.org/10.1016/j.meegid.2019.103922.

Data availability

The datasets generated and analyzed during the current study are available from the corresponding author upon reasonable request. Only the miRNA microarray data and mRNA sequencing data are not publicly available because these data contain unpublished information.

Author contributions

LG and JG contributed to the data analysis and the writing of the manuscript. YL contributed to the drafting of the manuscript. RL, QX and ZL contributed to the data collection and laboratory work. XF contributed to the conception of the idea and design. All authors read and approved the manuscript.

Acknowledgments

This study was supported by the National Natural Science Foundation of China (No. 31660040), Innovating Project of Guangxi Graduate Education and YCBZ2014027 from Guangxi Education Department, Young Scientist Foundation of Guangxi Medical University (Grant No. GXMUYSF201525), and Promotion Ability Project of Young Teachers in Guangxi Universities (Grant No. 2018KY0138). The funders played no role in the study design, data collection and analysis, or preparation of the manuscript.

Conflict of interests

The authors have no potential conflicts of interest to declare with respect to the research, authorship, and/or publication of this article.

References

Bauer, D.L.V., Tellier, M., Martinez-Alonso, M., Nojima, T., Proudfoot, N.J., Murphy, S., et al., 2018. Influenza virus mounts a two-pronged attack on host RNA polymerase II transcription. Cell Rep. 23 (7), 2119–2129 e2113. https://doi.org/10.1016/j.celrep.2018.04.047.

Blaise, S., de Parseval, N., Benit, L., Heidmann, T., 2003. Genomewide screening for fusogenic human endogenous retrovirus envelopes identifies syncytin 2, a gene conserved on primate evolution. Proc. Natl. Acad. Sci. U. S. A. 100 (22), 13013–13018. https://doi.org/10.1073/pnas.2132646100.

Blaise, S., Ruggieri, A., Dewannieux, M., Cosset, F.L., Heidmann, T., 2004. Identification of an envelope protein from the FRD family of human endogenous retroviruses (HERV-FRD) conferring infectivity and functional conservation among simians. J. Virol. 78 (2), 1050–1054.

Chen, F., Palem, J., Balish, M., Figliozzi, R., Ajavon, A., Hsia, S.V., 2014. A novel thyroid hormone mediated regulation of HSV-1 gene expression and replication is specific to neuronal cells and associated with disruption of chromatin condensation. SOJ Pharm. Pharm. Sci. 1 (1).

Cui, L., Qi, Y., Li, H., Ge, Y., Zhao, K., Qi, X., et al., 2011. Serum microRNA expression profile distinguishes enterovirus 71 and coxsackievirus 16 infections in patients with hand-foot-and-mouth disease. PLoS ONE 6 (11), e27071. https://doi.org/10.1371/journal.pone.0027071.

Czabotar, P.E., Martin, S.R., Hay, A.J., 2004. Studies of structural changes in the M2 proton channel of influenza a virus by tryptophan fluorescence. Virus Res. 99 (1), 57–61.

Deschamps, T., Bazot, Q., Leske, D.M., MacLeod, R., Mompelat, D., Tafforeau, L., et al., 2017. Epstein-Barr virus nuclear antigen 1 interacts with regulator of chromosome condensation 1 dynamically throughout the cell cycle. J. Gen. Virol. 98 (2), 251–265. https://doi.org/10.1099/jgv.0.000681.

Ducatez, M.F., Hause, B., Stigger-Rosser, E., Darnell, D., Corzo, C., Juleen, K., et al., 2011. Multiple reassortment between pandemic (H1N1) 2009 and endemic influenza viruses in pigs, United States. Emerg. Infect. Dis. 17 (9), 1624–1629. https://doi.org/10.3201/eid1709.110338.

El-Ekiaby, N.M., Mekky, R.Y., Riad, S.E., Elhelw, D.S., El-Sayed, M., Esmat, G., et al., 2017. miR-148a and miR-30a limit HCV-dependent suppression of the lipid droplet protein, ADRP, in HCV infected cell models. J. Med. Virol. 89 (4), 653–659. https://doi.org/10.1002/jmv.24677.

Fan, X., Zhu, H., Zhou, B., Smith, D.K., Chen, X., Lam, T.T., et al., 2012. Emergence and dissemination of a swine H3N2 reassortant influenza virus with 2009 pandemic H1N1 genes in pigs in China. J. Virol. 86 (4), 2375–2378. https://doi.org/10.1128/JVI.06824-11.

Fu, Y., Xu, W., Chen, D., Feng, C., Zhang, L., Wang, X., et al., 2015. Enterovirus 71 induces autophagy by regulating has-miR-30a expression to promote viral replication. Antivir. Res. 124, 43–53. https://doi.org/10.1016/j.antiviral.2015.09.016.

Garten, R.J., Davis, C.T., Russell, C.A., Shu, B., Lindstrom, S., Balish, A., et al., 2009. Antigenic and genetic characteristics of swine-origin 2009 a(H1N1) influenza viruses circulating in humans. Science 325 (5937), 197–201. https://doi.org/10.1126/science.1176225.

Grove, J., Huby, T., Stamataki, Z., Vanwolleghem, T., Meuleman, P., Farquhar, M., et al., 2007. Scavenger receptor BI and BII expression levels modulate hepatitis C virus infectivity. J. Virol. 81 (7), 3162–3169. https://doi.org/10.1128/JVI.02356-06.

Howard, W.A., Essen, S.C., Strugnell, B.W., Russell, C., Barass, L., Reid, S.M., et al., 2011. Reassortant pandemic (H1N1) 2009 virus in pigs, United Kingdom. Emerg. Infect. Dis. 17 (6), 1049–1052. https://doi.org/10.3201/eid/1706.101886.

Hummel, J., Kammerer, U., Muller, N., Avota, E., Schneider-Schaulies, S., 2015. Human endogenous retrovirus envelope proteins target dendritic cells to suppress T-cell activation. Eur. J. Immunol. 45 (6), 1748–1759. https://doi.org/10.1002/eji.201445366.

Kenmochi, N., Kawaguchi, T., Rozen, S., Davis, E., Goodman, N., Hudson, T.J., et al., 1998. A map of 75 human ribosomal protein genes. Genome Res. 8 (5), 509–523.

Kim, H., Lee, S.W., Baek, K.M., Park, J.S., Min, J.H., 2011. Continuous hypoxia attenuates paraquat-induced cytotoxicity in the human A549 lung carcinoma cell line. Exp. Mol. Med. 43 (9), 494–500. https://doi.org/10.3858/emm.2011.43.9.056.

Kim, D., Langmead, B., Salzberg, S.L., 2015. HISAT: a fast spliced aligner with low memory requirements. Nat. Methods 12 (4), 357–360. https://doi.org/10.1038/nmeth.3317.

Kitikoon, P., Sreta, D., Na Ayudhya, S.N., Wongphatcharachai, M., Lapkuntod, J., Prakairungnamthip, D., et al., 2011. Brief report: molecular characterization of a novel reassorted pandemic H1N1 2009 in Thai pigs. Virus Genes 43 (1), 1–5. https://doi.org/10.1007/s11262-011-0597-5.

Lam, W.Y., Yeung, A.C., Ngai, K.L., Li, M.S., To, K.F., Tsui, S.K., et al., 2013. Effect of avian influenza a H5N1 infection on the expression of microRNA-141 in human respiratory epithelial cells. BMC Microbiol. 13, 104. https://doi.org/10.1186/1471-2180-13-104.

Langmead, B., Salzberg, S.L., 2012. Fast gapped-read alignment with bowtie 2. Nat. Methods 9 (4), 357–359. https://doi.org/10.1038/nmeth.1923.

Li, X., Fan, P., Jin, J., Su, W., An, D., Xu, L., et al., 2013. Establishment of cell lines with increased susceptibility to EV71/CA16 by stable overexpression of SCARB2. Virol. J. 10, 250. https://doi.org/10.1186/1743-422X-10-250.

Liang, H., Lam, T.T., Fan, X., Chen, X., Zeng, Y., Zhou, J., et al., 2014. Expansion of genotypic diversity and establishment of 2009 H1N1 pandemic-origin internal genes in pigs in China. J. Virol. 88 (18), 10864–10874. https://doi.org/10.1128/JVI.01327-14.

Loveday, E.K., Svinti, V., Diederich, S., Pasick, J., Jean, F., 2012. Temporal- and strain-specific host microRNA molecular signatures associated with swine-origin H1N1 and avian-origin H7N7 influenza a virus infection. J. Virol. 86 (11), 6109–6122. https://doi.org/10.1128/JVI.06892-11.

Ma, W., Belisle, S.E., Mosier, D., Li, X., Stigger-Rosser, E., Liu, Q., et al., 2011. 2009 pandemic H1N1 influenza virus causes disease and upregulation of genes related to inflammatory and immune responses, cell death, and lipid metabolism in pigs. J. Virol. 85 (22), 11626–11637. https://doi.org/10.1128/JVI.05705-11.

Majer, A., Caligiuri, K.A., Gale, K.K., Niu, Y., Phillipson, C.S., Booth, T.F., et al., 2017. Induction of multiple miR-200/182 members in the brains of mice are associated with acute herpes simplex virus 1 encephalitis. PLoS ONE 12 (1), e0169081. https://doi.org/10.1371/journal.pone.0169081.

Makkoch, J., Poomipak, W., Saengchoowong, S., Khongnomnan, K., Praianantathavorn, K., Jinato, T., et al., 2016. Human microRNAs profiling in response to influenza a viruses (subtypes pH1N1, H3N2, and H5N1). Exp. Biol. Med. (Maywood) 241 (4), 409–420. https://doi.org/10.1177/1535370215611764.

Martinez-Alonso, M., Hengrung, N., Fodor, E., 2016. RNA-free and ribonucleoprotein-associated influenza virus polymerases directly bind the Serine-5-phosphorylated carboxyl-terminal domain of host RNA polymerase II. J. Virol. 90 (13), 6014–6021. https://doi.org/10.1128/JVI.00494-16.

Mirabello, L., Macari, E.R., Jessop, L., Ellis, S.R., Myers, T., Giri, N., et al., 2014. Whole-exome sequencing and functional studies identify RPS29 as a novel gene mutated in multicase diamond-Blackfan anemia families. Blood 124 (1), 24–32. https://doi.org/10.1182/blood-2013-11-540278.

Morozov, V.A., Dao Thi, V.L., Denner, J., 2013. The transmembrane protein of the human endogenous retrovirus–K (HERV-K) modulates cytokine release and gene expression. PLoS ONE 8 (8), e70399. https://doi.org/10.1371/journal.pone.0070399.

Ngo, L.T., Hiromoto, Y., Pham, V.P., Le, H.T., Nguyen, H.T., Le, V.T., et al., 2012. Isolation of novel triple-reassortant swine H3N2 influenza viruses possessing the hemagglutinin and neuraminidase genes of a seasonal influenza virus in Vietnam in 2010. Influenza Other Respir. Viruses 6 (1), 6–10. https://doi.org/10.1111/j.1750-2659.2011.00267.x.

Oymans, J., Te Velthuis, A.J.W., 2018. A mechanism for priming and realignment during influenza a virus replication. J. Virol. 92 (3). https://doi.org/10.1128/JVI.01773-17.

Pereda, A., Cappuccio, J., Quiroga, M.A., Baumeister, E., Insarralde, L., Ibar, M., et al., 2010. Pandemic (H1N1) 2009 outbreak on pig farm, Argentina. Emerg. Infect. Dis. 16 (2), 304–307. https://doi.org/10.3201/eid1602.091230.

Plafker, K., Macara, I.G., 2000. Facilitated nucleocytoplasmic shuttling of the ran binding protein RanBP1. Mol. Cell. Biol. 20 (10), 3510–3521.

Roberts, A., Pachter, L., 2013. Streaming fragment assignment for real-time analysis of sequencing experiments. Nat. Methods 10 (1), 71–73. https://doi.org/10.1038/nmeth.2251.

Roggen, E.L., Soni, N.K., Verheyen, G.R., 2006. Respiratory immunotoxicity: an in vitro assessment. Toxicol. in Vitro 20 (8), 1249–1264. https://doi.org/10.1016/j.tiv.2006.03.009.

Samji, T., 2009. Influenza a: understanding the viral life cycle. Yale J. Biol. Med. 82 (4), 153–159.

Shen, H., Lu, S., Dong, L., Xue, Y., Yao, C., Tong, C., et al., 2018. Hsa-miR-320d and hsa-miR-582, miRNA biomarkers of aortic dissection, regulate apoptosis of vascular smooth muscle cells. J. Cardiovasc. Pharmacol. 71 (5), 275–282. https://doi.org/10.1097/FJC.0000000000000568.

Singh, A.K., Rooge, S.B., Varshney, A., Vasudevan, M., Bhardwaj, A., Venugopal, S.K., et al., 2018. Global microRNA expression profiling in the liver biopsies of hepatitis B virus-infected patients suggests specific microRNA signatures for viral persistence and hepatocellular injury. Hepatology 67 (5), 1695–1709. https://doi.org/10.1002/hep.29690.

Smith, G.J., Vijaykrishna, D., Bahl, J., Lycett, S.J., Worobey, M., Pybus, O.G., et al., 2009. Origins and evolutionary genomics of the 2009 swine-origin H1N1 influenza a epidemic. Nature 459 (7250), 1122–1125. https://doi.org/10.1038/nature08182.

Starick, E., Lange, E., Fereidouni, S., Bunzenthal, C., Hoveler, R., Kuczka, A., et al., 2011. Reassorted pandemic (H1N1) 2009 influenza a virus discovered from pigs in Germany. J. Gen. Virol. 92 (Pt 5), 1184–1188. https://doi.org/10.1099/vir.0.028662-0.

Stark, T.J., Arnold, J.D., Spector, D.H., Yeo, G.W., 2012. High-resolution profiling and analysis of viral and host small RNAs during human cytomegalovirus infection. J. Virol. 86 (1), 226–235. https://doi.org/10.1128/JVI.05903-11.

Trapnell, C., Williams, B.A., Pertea, G., Mortazavi, A., Kwan, G., van Baren, M.J., et al., 2010. Transcript assembly and quantification by RNA-Seq reveals unannotated transcripts and isoform switching during cell differentiation. Nat. Biotechnol. 28 (5), 511–515. https://doi.org/10.1038/nbt.1621.

Tuddenham, L., Jung, J.S., Chane-Woon-Ming, B., Dolken, L., Pfeffer, S., 2012. Small RNA deep sequencing identifies microRNAs and other small noncoding RNAs from human herpesvirus 6B. J. Virol. 86 (3), 1638–1649. https://doi.org/10.1128/JVI.05911-11.

Weingartl, H.M., Berhane, Y., Hisanaga, T., Neufeld, J., Kehler, H., Emburry-Hyatt, C., et al., 2010. Genetic and pathobiologic characterization of pandemic H1N1 2009 influenza viruses from a naturally infected swine herd. J. Virol. 84 (5), 2245–2256. https://doi.org/10.1128/JVI.02118-09.

Wu, Z., Hao, R., Li, P., Zhang, X., Liu, N., Qiu, S., et al., 2013. MicroRNA expression profile of mouse lung infected with 2009 pandemic H1N1 influenza virus. PLoS ONE 8 (9), e74190. https://doi.org/10.1371/journal.pone.0074190.

Yamayoshi, S., Iizuka, S., Yamashita, T., Minagawa, H., Mizuta, K., Okamoto, M., et al., 2012. Human SCARB2-dependent infection by coxsackievirus A7, A14, and A16 and enterovirus 71. J. Virol. 86 (10), 5686–5696. https://doi.org/10.1128/JVI.00020-12.

Zhang, Y., Shao, L., 2018. Decreased microRNA-140-5p contributes to respiratory syncytial virus disease through targeting Toll-like receptor 4. Exp. Ther. Med. 16 (2), 993–999. https://doi.org/10.3892/etm.2018.6272.

Zhou, Z.D., Bao, L., Liu, D.G., Li, M.Q., Ge, Y.Z., Huang, Y.L., et al., 2003. Low content of protein S29 in ribosomes of human lung cancer cell line a549: detected by two-dimensional electrophoresis. Protein Pept. Lett. 10 (1), 91–97.